

Lateral soil resistance to an untrenched pipeline under the action of ocean currents

F.P. Gao

Key Laboratory for Hydrodynamics and Ocean Engineering, Institute of Mechanics, Chinese Academy of Sciences, Beijing, China

S.M. Yan

Key Laboratory for Hydrodynamics and Ocean Engineering, Institute of Mechanics, Chinese Academy of Sciences, Beijing, China

China Petroleum Pipeline Engineering Corporation, Langfang, China

E.Y. Zhang

CNOOC Research Center, Beijing, China

Y.X. Wu

Key Laboratory for Hydrodynamics and Ocean Engineering, Institute of Mechanics, Chinese Academy of Sciences, Beijing, China

X. Jia

CNOOC Research Center, Beijing, China

ABSTRACT: A plane-strain finite element model is proposed to investigate the pipe-soil interaction mechanisms for the partially embedded pipe with two kinds of constraint conditions, i.e. freely-laid pipe and anti-rolling pipe. The numerical model is verified with updated mechanical-actuator experiments. The magnitude of lateral-soil-resistance coefficient for the examined anti-rolling pipes is much larger than that for the freely-laid pipes, indicating the end-constraint condition affects significantly the lateral stability of the untrenched pipeline in ocean currents. Parametric study indicates that the variation of lateral-soil-resistance coefficient with the dimensionless submerged weight of pipe is affected greatly by the internal friction angle of soil, pipe-soil friction coefficient, etc.

1 INTRODUCTION

To avoid the occurrence of pipeline on-bottom (lateral) instability, i.e. the breakout of the pipe from its original site, the seabed must provide enough soil resistance to balance the hydrodynamic loads upon the untrenched pipeline. For pipeline geotechnical engineers, one of the main concerns for pipeline on-bottom stability design is to properly predict the ultimate soil resistance in the severe ocean environments, and to further determine the thickness of coating layers based on nominal pipe weight (Det Norske Veritas 2007).

In the past few decades, the pipe-soil interactions have attracted much interest from pipeline researchers and designers. Numerous experimental studies on wave-induced pipe instability have been carried out with 1g mechanical actuators (e.g., Wagner et al. 1987; Palmer et al. 1988), with centrifugal pipe-soil interaction tests on calcareous sand (e.g. Zhang et al. 2002), and with flume hydrodynamic simulations (e.g. Gao et al. 2003; Teh et al. 2003). Several empirical

“pipe-soil” or “wave-pipe-soil” interaction models were developed to improve the conventional Coulomb friction theory. Some reviews on pipeline geotechnics and pipe-soil interactions have been made recently by Cathie et al. (2005), White and Randolph (2007), etc. Note that the aforementioned studies mainly focused on the pipeline on-bottom stability subjected to ocean waves.

As the oil and gas exploitation moving into deeper waters, ocean current becomes the prevailing hydrodynamic load for on-bottom stability of submarine pipelines. Although the pipe on-bottom stability in currents seems less complicated than in waves, till now, the underlying physical mechanism has not been well revealed (Gao et al. 2007).

To further explore the mechanism of pipeline on-bottom stability in ocean currents, a plane-strain finite element model is proposed and verified with the mechanical-actuator tests. The ultimate lateral soil resistance to the untrenched pipes with two kinds of constraint conditions, i.e. freely-laid pipes and anti-rolling pipes, is investigated numerically.

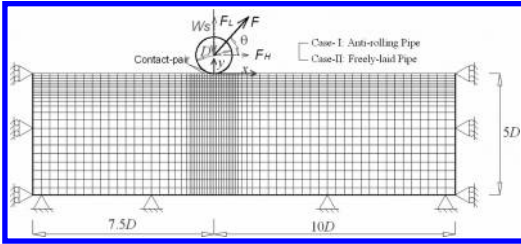


Figure 1. Typical plane-strain finite element mesh (not in scale) and boundary conditions for pipe lateral stability analyses.

2 DEVELOPMENT OF A PLANE-STRAIN PIPE-SOIL INTERACTION MODEL

2.1 The finite element model

2.1.1 Finite element mesh and boundary conditions
As the length of a submarine pipeline is much larger than its diameter, the pipeline lateral stability can be treated as a plane-strain problem. A plane-strain finite element model is proposed for simulating the breakout of the pipeline from its original site. The typical finite element mesh is illustrated in Figure 1.

The boundary conditions are set as follows: (1) at the left and right boundary, no displacement in the x direction takes place; (2) the bottom boundary is fixed, i.e. the displacement and rotation are not permitted; (3) at the pipe-soil interface, the contact-pair algorithm provided in the ABAQUS software (Hibbitt, Karlsson and Sorensen Inc, 2006) is adopted to simulate the moving pipe along the deformable soil. The non-contact soil surface is treated as a free boundary. In the numerical modelling of the pipeline losing on-bottom stability, it is crucial to properly describe the contact conditions between the pipe and the neighbouring soil. The pipe-soil friction is defined by the Penalty Function with the advantage that it guarantees the positive definiteness of sparse matrix in the calculation. In order to avoid large distortion of finite elements causing the calculation misconvergence, the self-adaptive mesh technology is employed.

To obtain high calculation efficiency, the finite element mesh gets more refined at closer proximity to the pipe. Based on the results of a series of trial calculations, the width of the numerical model is set as $17.5D$ and the depth as $5D$, and the pipeline is located at $x = 7.5D$ (D is the pipeline diameter), see Figure 1.

2.1.2 The end-constraint and the simulation of ocean current loading on the pipeline

For a long-distance laid pipeline, the on-bottom stability of the pipeline at its separate sections is different. Due to the constraints from risers and the pipeline own anti-torsion rigidity, the pipeline movement is neither purely parallel nor purely rotational. As such, the following two end-constraint conditions are taken account in the present study: Case I: Anti-rolling pipe.

Pipeline's rolling is restricted, but pipeline can move freely in horizontal and vertical directions; Case II: Freely-laid pipe. The pipe may rotate around its axis without any end constraint.

When a pipeline is laid on the seabed under the action of ocean currents, there exists a dynamic balance between the submerged weight of the pipe, the hydrodynamics forces (including the horizontal drag force F_D and the vertical lift force F_L), and the soil resistances. When the ultimate lateral soil resistance is not able to balance the horizontal drag force, the pipe would breakout from its original site, i.e. the lateral instability occurs.

To efficiently simulate the ocean currents induced hydrodynamic loads upon a submarine pipe-line is crucial for evaluating pipeline lateral on-bottom stability. According to Morison's equation, the horizontal and lift (vertical) components of the steady flow induced horizontal drag force and vertical lift force are expressed as $F_D = 0.5C_D\rho_wDU^2$, $F_L = 0.5C_L\rho_wDU^2$, respectively. Herein, C_D is the drag coefficient, C_L is the lift coefficient, ρ_w is the mass density of water, U is the effective water particle velocity. The variations of the drag and lift coefficients, C_D and C_L , with the Reynolds number (Re) for various values of pipe surface roughness have been obtained by Jones (1978). The resultant hydrodynamics force upon the pipe is obliquely upwards with the inclination angle:

$$\theta = \arctan(F_L/F_D) \approx \arctan(C_L/C_D) \quad (1)$$

Referring to the experimental results by Jones (1978), the inclination angle (θ) is approximately between $53^\circ - 57^\circ$. It is therefore reasonable to apply an inclined force in the θ direction to simulate the hydrodynamic loads on the pipe in steady ocean currents.

2.1.3 Constitutive model for soils and the material properties

The sandy soil under drained conditions can be essentially assumed to behave as an elastic $c-\phi$ material (e.g. Mohr-Coulomb or D-P material). The seabed soil is simulated with the well-known Drucker-Prager (D-P) elastoplasticity constitutive model. In the simulations, the parameters of soil are chosen as follows: Young's modulus $E = 0.18$ MPa, Poisson's ratio $\nu = 0.32$, the cohesion $c = 0$, the buoyant unit weight of the soil $\gamma' = 9.3 \times 10^3$ N/m³, the values of soil internal friction angle ϕ are various for the parametric study in Section 3.1.

As aforementioned, the pipe is treated as a rigid cylinder with outer diameter $D = 0.15$ m (same as the test pipes). The submerge weight of the pipe per meter (W_s) and the pipe-soil friction coefficient (μ) are various for parametric studies in Section 3. Due to that the stiffness of the steel pipeline with concrete cover is normally larger than that of the soil, the wall of the pipeline is regarded as a rigid cylinder in this finite element analysis.

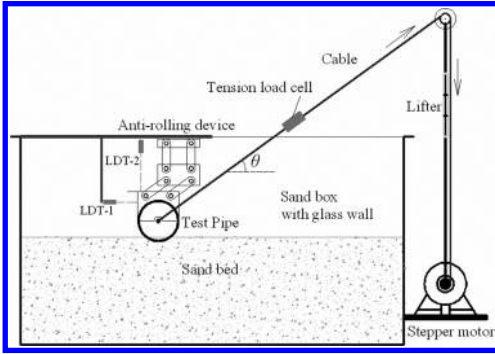


Figure 2. Experimental setup for pipe lateral stability.

2.2 Verification of numerical model

To verify the proposed numerical model, an updated experimental facility by employing the mechanical-actuator simulation method has recently been designed and constructed, as depicted in Fig. 2. The facility mainly consists of a sand box with glass wall, a mechanical-actuator, and the measurement system, etc.. In the sand box (2 m long, 0.5 m wide and 0.6 m deep), a saturated sand-bed with certain relative density can be prepared by employing the sand-raining technique. In the mechanical actuator system, a stepper motor was capable of generating inclined force onto the test pipe via a cable passing through a fixed pulley, for simulating steady currents induced drag force and lift force on the pipeline. Meanwhile, a lifter was used to adjust the inclination angle, which was maintained in the range of $53^\circ \sim 57^\circ$ according to the above analyses.

Figure 3(a) illustrates typical development of lateral soil resistance and the corresponding vertical pipe-soil contact force for an anti-rolling pipe when losing lateral stability. With the increase of horizontal displacement (S_x) during the pipe losing lateral stability, the horizontal lateral soil resistance (F_H) increases gradually to its maximum value ($F_u = 0.10$ kN/m) when the additional settlement is nearly fully developed according to the experimental observation. Meanwhile, the corresponding vertical pipe-soil contact force ($W_S - F_H \tan\theta$) decreases gradually to its minimum value (0.085 kN/m). The FEM numerical results match well with the test results. Figure 3(b) shows the numerical results of plastic deformation beneath the anti-rolling pipe while losing lateral stability. It is indicated that the shear band is distributed underneath the deformed soil layer; meanwhile, the soil just in front of the moving pipe upheaves obviously (see Figure 3b).

The variation of ultimate lateral soil resistance (F_u) with the vertical pipe-soil contact force ($W_S - F_u \tan\theta$) is given in Figure 4, indicating the numerical and the experimental results are quite comparable. The ultimate lateral soil resistance increases linearly with the vertical pipe-soil contact force. The proposed FEM model is capable of predicting the lateral resistance for the untrenched pipeline on-bottom instability.

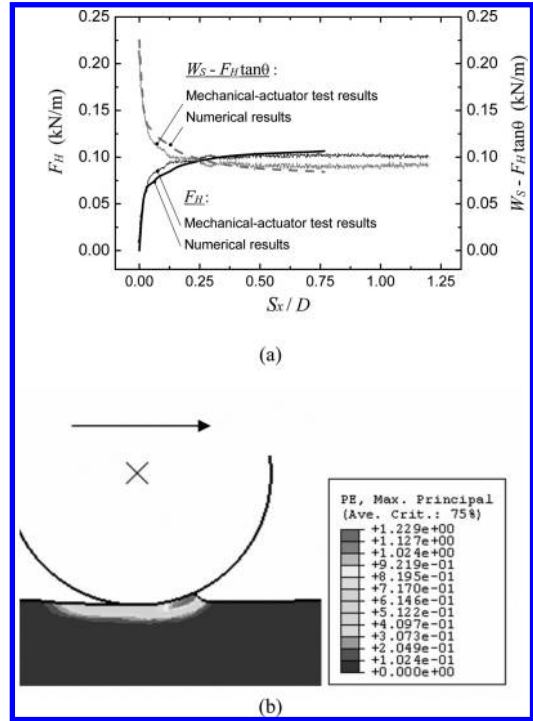


Figure 3. (a) Development of lateral soil resistance and the corresponding vertical pipe-soil contact force for an anti-rolling pipe when losing lateral stability: Comparison between numerical and experimental results; (b) Plastic deformation beneath the anti-rolling pipe while losing lateral stability ($D = 0.15$ m, $\mu = 0.7$, $W_S = 0.225$ kN/m, $\phi = 26.7^\circ$).

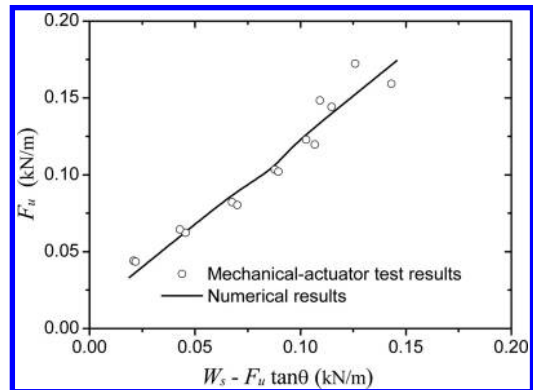


Figure 4. Variation of ultimate lateral soil resistance with vertical pipe-soil contact force: Comparison between the numerical and the experimental results ($D = 0.15$ m, $\mu = 0.7$, $\phi = 26.7^\circ$).

3 NUMERICAL RESULTS AND ANALYSES

In the process of a pipeline losing lateral stability under the action of ocean currents, the soil plastic deformation beneath the untrenched pipeline may be

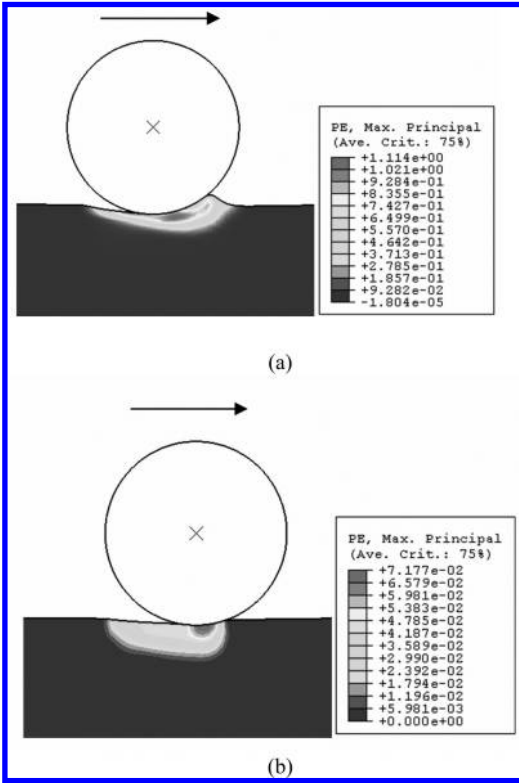


Figure 5. Plastic deformation beneath the pipe while losing lateral stability: (a) Anti-rolling pipe; (b) Freely-laid pipe ($D = 0.15$ m, $W_s = 0.439$ kN/m, $\mu = 0.7$, $\phi = 20^\circ$).

created due to the intensive pipe-soil interaction. Figure 5(a) and (b) illustrate the plastic strain in the proximity of an anti-rolling pipeline and that of a freely-laid pipeline, respectively. It is indicated that, the end-constraint condition has much influence on the distribution of the plastic strain zone in the soil. For the anti-rolling pipeline, an obvious shear strain band may be formed in the underlying soil layer, and soil upheave occurs in front of the moving pipeline (see Figure 5(a)). Nevertheless, for the freely-laid pipeline, the smaller plastic-strain zone is created just underneath the rolling pipeline (see Figure 5(b)).

As discussed above, many factors influencing the pipe-soil interaction could be incorporated in the proposed finite element model. In the following sections, the effects of soil internal friction angle and the pipe-soil friction coefficient on the on-bottom stability of the pipelines with two kinds of end-constraint will be further investigated numerically.

3.1 Effects of soil internal friction angle

For better understanding the pipe-soil interaction mechanism for on-bottom stability, a lateral-soil-resistance coefficient (η) is proposed, whose physical meaning is the ratio of the ultimate value of the

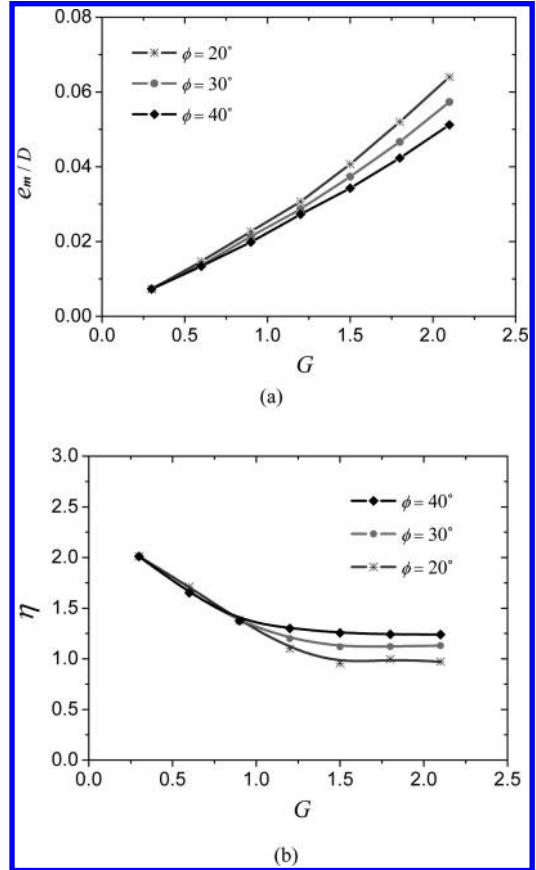


Figure 6. Lateral stability of anti-rolling pipes for various values of internal friction angle: (a) e_m/D vs. G ; (b) η vs. G ($D = 0.15$ m, $\mu = 0.7$).

horizontal lateral soil resistance to the corresponding vertical pipe-soil contact force, i.e.

$$\eta = \frac{F_u}{W_s - F_u \tan \theta} \quad (2)$$

The commonly-used dimensionless submerged weight (G) of the pipe is

$$G = \frac{W_s}{\gamma' D^2} \quad (3)$$

where γ' is the buoyant unit weight of the saturated sand.

Both the experimental and numerical results show that, in addition to the initial embedment due to self-weight of the pipe in the process of losing lateral stability, some additional settlement may be developed while the horizontal lateral soil resistance increases gradually to its maximum value.

Figure 6(a) and (b) give the variation of maximum pipe settlement (e_m/D) with the dimensionless pipe submerged weight (G) and that of the corresponding lateral soil resistance coefficient (η) with

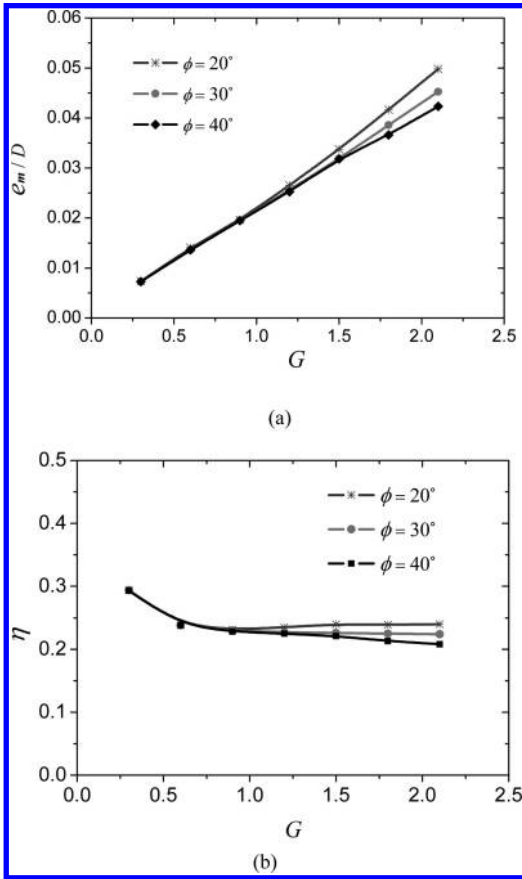


Figure 7. Lateral stability of freely-laid pipes for various values of internal friction angle: (a) e_m/D vs. G ; (b) η vs. G ($D = 0.15$ m, $\mu = 0.7$).

G for various values of soil internal frictional angles for the Case of anti-rolling pipeline with a given diameter ($D = 0.15$ m). The maximum pipeline settlements (e_m/D) in the process of pipeline losing stability increase approximately linearly with the increase of G . For the same value of G , e_m/D increases with the decrease of soil internal friction angle, especially for the larger pipeline submerged weights (see Figure 6(a)). The lateral-soil-resistance coefficient (η) decreases gradually to a constant value with the increase of G . The effect of soil internal friction angle on η gets more significant with increasing submerged weight of the pipeline.

Similarly, the variation of e_m/D with G and that of η with G for the case of freely-laid pipelines are given in Figure 7(a) and (b). Compared with the case of anti-rolling pipelines (see Figure 6), the relationships between e_m/D and G for the freely-laid pipes follow similar trends, but the maximum settlements are somewhat less in magnitude. Unlike the case of anti-rolling pipe, the effect of ϕ on the variation of η with G for the freely-laid pipeline is different, i.e. η decreases with the increase of ϕ for a fixed value of G (e.g.

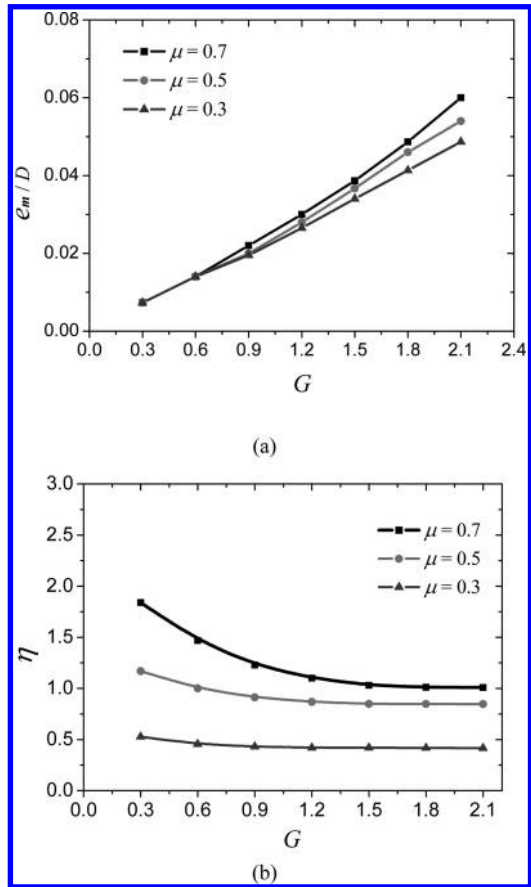


Figure 8. Effects of pipe-soil friction coefficients on the lateral stability of anti-rolling pipes: (a) e_m/D vs. G ; (b) η vs. G ($D = 0.15$ m, $\phi = 26.7^\circ$).

$G > 1.0$, see Figure 7(b)). This may attribute to that the pipe settles shallower into the soil with bigger internal friction angle, and that the freely-laid pipe tends to roll away from its original site. Note that the range of η for the examined anti-rolling pipes is between 1.0 ~ 2.0 (see Figure 6(b)), but that for the freely-laid pipes only between 0.2~0.3 (see Figure 7(b)). Therefore, the end-constraints have significant influence on the lateral stability of the untrenched pipeline in ocean currents.

3.2 Effects of pipe-soil friction coefficient

The submarine pipeline is usually constructed with concrete cover. As imagined, the pipe-soil friction coefficient may affect the lateral stability of the pipeline.

Figure 8 (a) and (b) give the variation of e_m/D with G and that of η with G for various values of pipe-soil friction coefficient (μ), respectively. For the case of anti-rolling pipes, the increase of μ brings an increase of maximum settlement in the process of pipe losing lateral stability (see Figure 8(a)). The effect of

pipe-soil friction coefficient is more obvious for the smaller value of G . Its effect on the variation of η with G gets less with the decrease of μ (see Figure 8(b)).

4 CONCLUDING REMARKS

As the offshore oil & gas exploitation goes into deeper waters, ocean current becomes the prevailing hydrodynamic load for on-bottom stability of submarine pipelines. In this paper, a finite element model is proposed and verified with the updated mechanical-actuator experiments. Parametric study is made to investigate the pipe-soil interaction mechanism for the current-induced pipeline lateral instability. The following conclusions can be drawn:

- The finite element model can effectively simulate the behaviour of pipeline losing lateral stability in ocean currents under two end-constraint conditions, i.e. the anti-rolling pipe and the freely-laid pipe. The ultimate lateral soil resistance can be obtained from the load vs. displacement curve.
- A lateral-soil-resistance coefficient (η) is presented for better understanding pipe-soil interaction mechanism. The value of η decreases gradually to a constant with the increase of G . The magnitude of η for the examined anti-rolling pipes is much larger than that for the freely-laid pipes, indicating the end-constraint condition affects significantly the lateral stability of the untrenched pipeline in ocean currents.
- For a certain case of end constraint (anti-rolling or freely-laid), the variation of η with G is affected by various parameters, including soil internal friction angle, pipe-soil friction coefficient, etc. The effect of pipe-soil friction coefficient is more obvious for the smaller value of G .
- When evaluating the capacity of lateral resistance, it would be beneficial to further examine and get correlation with the maximum pipeline penetration (including initial and additional settlement) and the development of the plastic-strain zone beneath the pipeline.

ACKNOWLEDGEMENTS

The work reported herein is financially supported by Knowledge Innovation Program of the Chinese Academy of Sciences (No. KJ CX2-YW-L02) and China National S&T Major Project (No. 2008ZX05026-005).

REFERENCES

- Cathie, D.N., Jaeck, C., Ballard J-C. & Wintgens, J-F., 2005. Pipeline geotechnics – state of the art. In: *Frontiers in Offshore Geotechnics: ISFOG 2005*. Eds: Gourvenec S. and Cassidy M., New York: Taylor & Francis, 95–114.
- Det Norske Veritas, 2007. *On-Bottom Stability Design of Submarine Pipelines*. Recommended Practice, DNV-RP-F109.
- Gao, F.P., Gu, X.Y. and Jeng, D.S., 2003. Physical Modeling of Untrenched Submarine Pipeline Instability. *Ocean Engineering*, 30 (10): 1283–1304. (SCI, EI)
- Gao, F.P., Yan, S.M., Yang, B. and Wu, Y. X., 2007. Ocean currents induced pipeline lateral stability on sandy seabed. *Journal of Engineering Mechanics*, ASCE, 133(10): 1086–1092.
- Hibbitt, Karlsson and Sorensen Inc, 2006. *ABAQUS Theory Manual*, Version 6.5–1.
- Jones, W.T., 1978. On-bottom pipeline stability in steady water currents. *Journal of Petroleum Technology*, Vol. 30, 475–484.
- Palmer, A. C., Steenfelt, J. S. and Jacobsen, V., 1988. Lateral resistance of marine pipelines on sand. *Proceedings of 20th Annual Offshore Technology Conference*, OTC 5853, 399–408.
- Teh, T.C. and Palmer, A.C. and Damgaard, J.S., 2003. Experimental study of marine pipelines on unstable and liquefied seabed. *Coastal Engineering*, 50, 1–2: 1–17.
- Wagner, D. A., Murff, J. D., Brennodden, H., and Sveegen, O., 1987. Pipe-soil interaction model. *Proceedings of Nineteenth Annual Offshore Technology Conference*, OTC 5504, 181–190.
- White, D.J. and Randolph, M.F., 2007. Seabed Characterisation and Models for Pipeline-Soil Interaction. *Proceedings of the Seventeenth International Offshore and Polar Engineering Conference*, Lisbon, 758–769.
- Zhang, J., Stewart, D. P., Randolph, M. F., 2002. Modeling of shallowly embedded offshore pipelines in calcareous sand. *Journal of Geotechnical and Geoenvironmental Engineering*, ASCE, Vol. 128, 363–371.